Apple bruise detect with hyperspectral imaging technique

Rui Zhou (周 睿), Manping Ye (叶满萍), and Huacai Chen (陈华才)*

Zhejiang Province Modern Measurement Instrument and Technology Key Laboratory, College of Optical and Electronic Technology, China Jiliang University, Hangzhou 310018, China

**Corresponding author: cjluoptic@163.com*

Received September 30, 2013; accepted October 19, 2013; posted online February 27, 2014

There is a need to develop a non-destructive and fast detection method for bruising of fruits because the injuries lower quality of fruits, which lead to economic loss. In this paper, we propose a method to detect the bruise on apple surface with hyperspectral imaging technique. A hyperspectral image system consisting of a CCD digital camera, a line scanning spectrometer and a movable platform is designed to acquire the hyperspectral images of injured apples. Two models are established to distinguish the injured area on the surface from the normal area based on image processing technique with spatial clustering and Spectral Angle Mapper Classification (SAM), respectively. The discrimination accuracy of the SAM model is up to 100%, which is much higher than the spatial clustering model.

OCIS codes: 110.4234, 100.2960, 300.6170.

doi: 10.3788/COL201412.S11101.

The surface of fruits might get injured by external force during the process of picking or transportation. Sometimes, the slight bruise may not be visible, but it will turn brown and even leads to the decay of the whole fruit as time goes[1]. So, finding or developing a rapid, effective method to detect slight injuries of fruits has become one of the hottest topics.

Although the slightly injured tissues seem very similar to normal tissues, certain changes do happen in the internal injured tissues, and these changes can be detected by spectral response under certain wavelengths. Hyperspectral imaging technique is a combination of conventional imaging technique and spectral technique, which can simultaneously give information about image and spectrum of the samples[2]. Recently, this technique has been used in nondestructive quality test of agricultural and animal products[3–6]. Hence, this technique is also appropriate to detect the slight injuries on fruits[7,8].

In this paper, we proposed a method to detect the bruise on apple surface with hyperspectral imaging technique and image processing technique. This technique helps know about both the spectral and image information to discriminate the injured tissues from normal tissues. Two rapid discrimination models were established and compared.

Shaanxi Fuji apples were bought from supermarket, cleaned and artificially injured and kept in the refrigerator for image acquisition.

Figure 1 depicts the hyperspectral image acquisition system. The system is composed of five parts: (i) a CCD digital camera (Kappa DX4 285FW), (ii) a line scanning spectrometer (NI-IMAQ IEEE 1394 IIDC digital camera), (iii) light sources, (iv) a servo movable platform for samples, and (v) a controller for the platform (WNSC400 motion controller). Spectral images were collected and analyzed using data software (spectral image system). The halogen lamp was used as the light source; the spectral range was 400–1000 nm and spatial resolution was 50 μm.

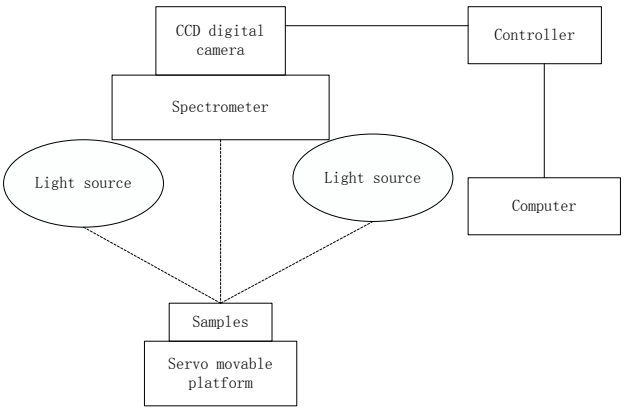

Fig. 1. Hyperspectral image acquisition system.

In order to ensure good image quality, the exposure time of the digital camera needs to be adjusted before collecting the hyperspectral images. To avoid distortion of image size or spatial resolution, the speed of the movable platform also needs to be adjusted according to the scan frequency of the digital camera.

Owing to the uneven distribution under different wavelengths of the light-source intensity and the existence of dark current, the camera needs to be calibrated prior to collecting the spectral images. Initially, the standard white board is placed on the sample platform, the position and intensity of the light sources are adjusted, and the light field data are obtained. Then, the digital camera lens is covered and the dark field data are obtained. These spectral images are calibrated automatically using the above-mentioned software. The equation used for calibration is

$$R = \frac{Sample - Dark}{White - Dark}, \tag{1}$$

where 'R' is the relative image after calibration; 'Sample' is the original image of the sample; 'Dark' is the image under dark current; 'White' is the reference image or the image under standard white board.

After the original image of apple sample is obtained (Fig. 2), a few points in the normal region and injured region are randomly chosen (Fig. 3), and the curve of spectral intensity versus wavelength of each chosen point are exported (Fig. 4). Meanwhile, several single-wavelength spectral images of the sample in near infrared region were obtained (wavelength region was set at 800–1000 nm, spectral interval at 25 nm; the result is shown in Fig. 5). Figure 4 shows three wavelengths with the most significant spectral difference between the injured region and the normal region, namely 925, 850 and 800 nm; and then three single-spectral images are used to generate a new image (Fig. 6) using image fusion technique. Finally, a spatial clustering method was used to distinguish the injured tissues from the normal tissues based on the new image.

Fig. 2. Original image of apple sample.

Fig. 3. The chosen points on sample.

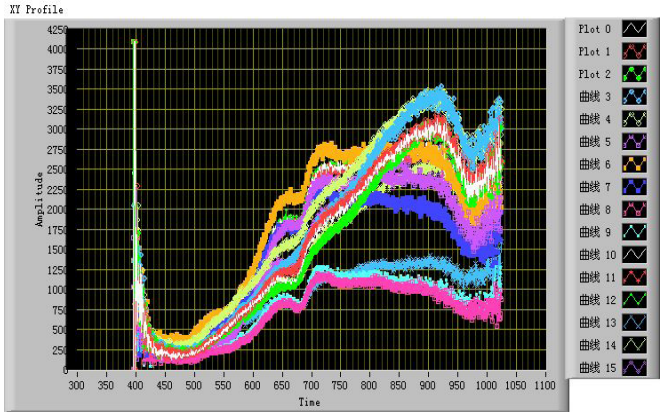

Fig. 4. Curve of spectral intensity versus wavelength of each chosen point.

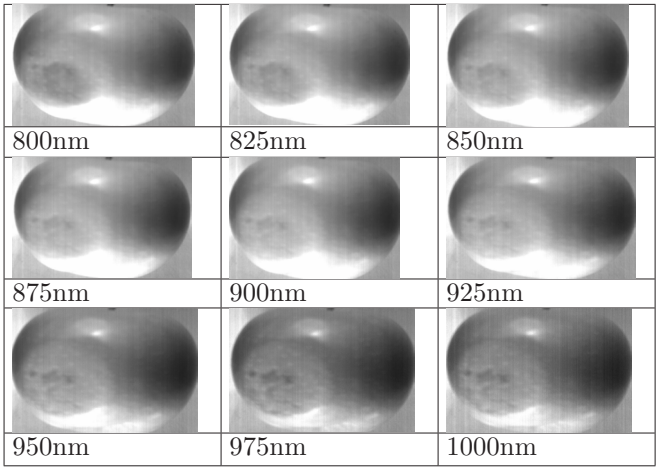

Fig. 5. Single-wavelength spectral images.

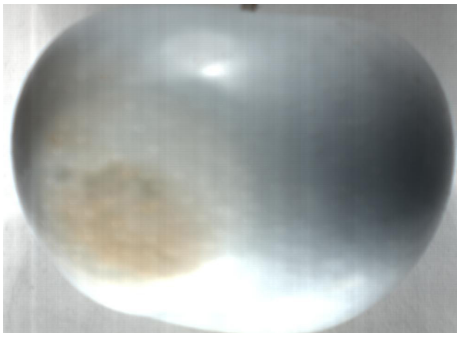

Fig. 6. Fusion image with three single-wavelength images (925nm, 850nm and 800nm).

In Figure 2, dark areas are seen on both left and right side. Actually, as in Fig. 7, only the region in the left circle was the injured, while the dark region in the right circle was just a shadow. So it is difficult to make out the difference between them by only the color of the images; hence, hyperspectral images are used instead. It is clear in Fig. 4 that the spectral intensity of points in normal region is apparently lower than that in the injured ones.

Figure 5 clearly indicates the difference between the injured region and normal region, but the dark area on right side still easily leads to a misjudgment. Compared to Fig. 5, the fusion image in Fig. 6 helps better to differentiate between normal regions and the injured ones.

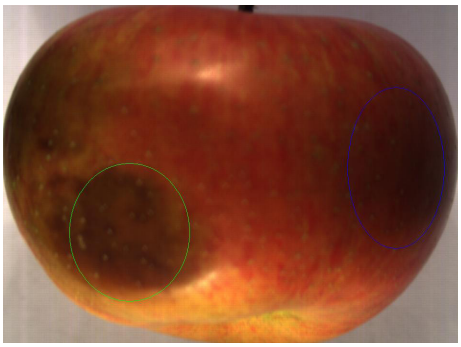

Fig. 7. Tissues in green circle were the injured ones while in blue circle were normal ones.

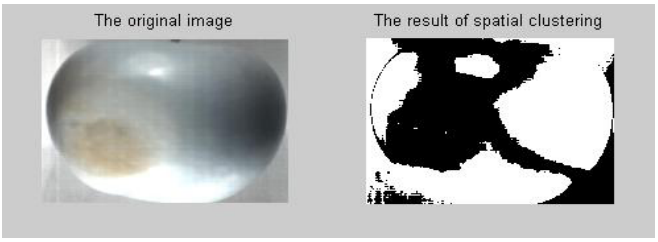

Fig. 8. The result of spatial clustering.

Fig. 9. The contrast district (within the yellow rectangle).

The difference was very clear and easy to discriminate in Fig. 6. Set the average spectral intensity of the chosen points from the injured region and normal region as the cluster centers, respectively, and performed spatial clustering on Fig. 6 through MATLAB. Fig. 8 shows the result, where the black part represented the injured tissue and the white part represented the normal tissue. Owing to the shadow of the light sources and the defects and restrictions of spatial clustering method, the results obtained were not very accurate, but still, they could be used to evaluate the quality level of apples.

The Spectral Angle Mapper (SAM) classification is an automated method for directly comparing image spectra with a known spectrum (usually determined in a lab or in the field with a spectrometer) or an end member[9]. This method treats both the questioned and knownspectra as vectors and calculates the spectral angle between them. This method is insensitive to illumination because the SAM algorithm uses only the vector direction and not the vector length. The result of the SAM classification is an image that shows the best match at each pixel. This technique has been used in several agricultural applications, including hyperspectral imagery for contaminant classification of chicken carcass[10], estimation of grain sorghum yield[11] and corn[12].

In this method, we also used the SAM classification method to discriminate the injured region from normal region. A small block in the injured region was chosen as the reference (Fig. 9), the spectral data of the reference were exported, the spectral similarity was checked and SAM was performed on the whole original image. The result is depicted in Fig. 10, the yellow parts are the injured regions.

Fig. 10. The result of SAM classification.

In conclusion, in this paper, two different models are established to distinguish the injured region from normal. First method is based on the image processing technique, in which spatial clustering is performed on an image fused by three single-wavelength spectral images to discriminate. The second method is based on the SAM classification method, which uses the spectral information of the apple samples to discriminate. The experiment results show that the former model is not perfect, but still it can be used to evaluate the quality level of the apple samples; while the SAM model is much more accurate and it can be used in high-precision detection.

The authors thank the support of The Project of Key Science and Technology Innovation Team of Zhejiang Province, No. 2010R50028 and Project of Special Fund for Quality Supervision and quarantine and quality inspection scientific research, No. 201310150.

References

1. J. W. Zhao, J. H. Liu, Q. S. Chen, and S. Vittayapadung, Trans. Chinese Soc. Agricultural Mach. **39,** 106 (2008).
2. B. X. Ma, Y. B. Ying, X. Q. Rao, and J. S. Gui, Spectrosc. Spectr. Anal. **29,** 1611 (2009).
3. H. H. Muhammed, Biosyst. Eng. **91,** 9 (2005).
4. E. Bauriegel, A. Giebel, M. Geyer, U. Schmidt, and W. B. Herppich, Comput. Electron. Agr. **75,** 304 (2011).
5. W. Wang, Y. K. Peng, and X. L. Zhang, Spectrosc. Spectral Anal. **30,** 411 (2010).
6. L. Wang, X. Y. Qiao, Y. E. Dong, M. Zhang, and Y. F. Shang, J. Appl. Optics. **30,** 639 2009.
7. J. Xing, C. Bravo, D. Moshou, H. Ramon, and J. D. Baerdemaeker, Comput. Electron. Agr. **52,** 11 (2006).
8. Q. Lv and M. Tang, Procedia Environ. Sci. **12,** 1172–1179 (2012).
9. F. A. Kruse, A. B. Lefkoff, J. W. Boardman, K. B. Heidebrecht, A. T. Shapiro, P. J. Barloon, and A. F. H. Goetz, Remote Sens. Environ. **44,** 145 (1993).
10. B. Park, W. R. Windham, K. C. Lawrence, and D. P. Smith, Biosyst. Eng. **96,** 323 (2007).
11. C. Yang, J. H. Everitt, and J. M. Bradford, Trans. ASAE., **51,** 729 (2008).
12. H. Yao, Z. Hruska, R. Kincaid, A. Ononye, R. L. Brown, and T. E. Cleveland, in *Proceedings of the Hyperspectral Image and Signal Processing: Evolution in Remote Sensing (WHISPERS)*, 1 (2010).